

# Fabrication and characterization of $\text{La}_{0.6}\text{Sr}_{0.4}\text{Co}_{0.2}\text{Fe}_{0.8}\text{O}_{3-\delta}$ (LSCF)- $\text{Ce}_{0.9}\text{Gd}_{0.1}\text{O}_{1.95}$ (GDC) composite thick film for anode supported solid oxide fuel cells

Atul P. Jamale<sup>1</sup> · C. H. Bhosale<sup>1</sup> · L. D. Jadhav<sup>2</sup>

Received: 8 June 2015 / Accepted: 30 September 2015 / Published online: 15 October 2015  
© Springer Science+Business Media New York 2015

**Abstract** Nowadays, the commercialization of solid oxide fuel cell (SOFC) is impeded by the chemical compatibility and polarization losses in association with electrode/electrolyte interface. Thus, to minimize these difficulties, the thick film of LSCF-GDC (50:50 wt%) composite was deposited onto GDC electrolyte to form perfect LSCF-GDC/GDC structure. The chemical compatibility of LSCF-GDC upon sintering of 1000 °C was confirmed from the X-ray diffraction studies. Typically, the film with 15 μm thickness possesses the porous structure, availing the free path for oxygen diffusion. The electrochemical impedance analysis of symmetric cell with LSCF-GDC as an electrode implies the relaxation of charge transfer and electrochemical reduction reaction with temperature. The NiO-GDC (30:70 wt%) supported SOFC with GDC and LSCF-GDC as an electrolyte and cathode, respectively was tested for their performance. The cell generates the maximum power density of 315 μWcm<sup>-2</sup> at 500 °C.

## 1 Introduction

A new potential electrochemical energy conversion SOFC device has attracted wide attention of the global research community due to its high electrical efficiency [1], fuel

flexibility [2], environmental friendly [3], and hence expected to be a promising energy conversion device of future. To date, tubular and planar designs are most studied SOFC modules. However, the SOFC configured in tubular design possesses lower power density and seems to be under high stresses due to its geometrically extended length and hence several failures during their operation [4]. Thus, the current research trend is to fabricate the electrolyte supported planar SOFCs as they possess OCV >1.1 V, while anode supported technology yields lower OCVs [5]. Another issue related with SOFC is its high operating temperature, which affects the chemical, mechanical and thermal durability. Therefore, main focus of the recent research is to lower the operating temperature to 500–700 °C by employing highly conducting GDC electrolyte instead of conventional YSZ. But, reducing operating temperature causes a sharp increase of internal cell resistance, especially in cathode [6]. Hence in present paper, two routes have been adopted to defeat the internal cell resistance viz; (1) increase of the number of reaction sites by forming composite cathode with ionically conducting GDC phase and (2) reducing thickness to a few microns by adoption of screen printing technique.

The processing parameters have significant impact on number of active sites [7], electrode/electrolyte interface and hence on the performance of SOFC. In the present work, the screen printing has been employed to deposit LSCF-GDC composite cathode. The technique has number of advantages over the other thick film deposition techniques. Such as it is easy, cost effective and thickness of film can be controlled over the range of 5–100 μm. Also, the films prepared with screen printing are porous in nature and hence it facilitates number of active sites for oxygen reduction reaction. For the potential application in the SOFC, the thickness of electrode should be controlled

✉ Atul P. Jamale  
jamaleatul@gmail.com

✉ L. D. Jadhav  
ldjadhav.phy@gmail.com

<sup>1</sup> Department of Physics, Shivaji University, Kolhapur 416004, India

<sup>2</sup> Electrochemical Energy Materials Laboratory, Department of Physics, Rajaram College, Kolhapur 416004, India

within 10–20  $\mu\text{m}$  and it is feasible with the screen printing technique [8].

## 2 Experimental

### 2.1 Formation of LSCF-GDC/GDC/LSCF-GDC structure

For symmetric cells, the GDC electrolytes were prepared by the solid state reaction route [9]. Here,  $\text{CeO}_2$  (Himedia, 99 %) and  $\text{Gd}_2\text{O}_3$  (Himedia, 99.90 %) were used as a starting materials. The initial powders were thoroughly mixed and ground in an ethanol medium for homogenization, and subsequently calcined at 700 °C for 2 h. The powder was then compacted under the co-axial hydraulic pressure of 110 MPa for 3 min and sintered at 1300 °C for 8 h to achieve a relative density of 93–96 %. The pellets were polished with silicon carbide 400 grit sandpaper to obtain smooth and parallel surface conditions.

The LSCF and GDC powders required for screen printing were obtained through glycine-nitrate process (GNP) at the glycine to nitrate ratio of 2:1 and 1.6:1, respectively [10, 11]. For GNP, the precursors were liquified in deionized water to obtain homogeneity at the molecular level. The entire solution was continuously stirred with heating on magnetic stirrer to obtain the viscous gel, which was kept on the pre-heated hot plate maintained at 400 °C. At 400 °C, the combustion reaction occurred spontaneously to form fine powder. Since the synthesized powder contains unusual residual impurities, the LSCF and GDC were calcined at 900 and 600 °C to get phase pure product with rhombohedral and cubic structure,

respectively. Thereafter, the LSCF and GDC powders were mixed together in ethanol medium in the weight ratio of 50:50 and ground for half an hour for homogenization. The slurry was formed by mixing the proper amounts of LSCF-GDC powder and organic vehicle (8 wt% ethyl cellulose + 92 % terpineol) to achieve sufficient viscosity. Finally, the LSCF-GDC slurry was applied onto both sides of GDC with 140 screen printing mesh, and subsequently fired at 1000 °C for 2 h. The procedure followed during the fabrication of symmetric cell is schematically shown in Fig. 1.

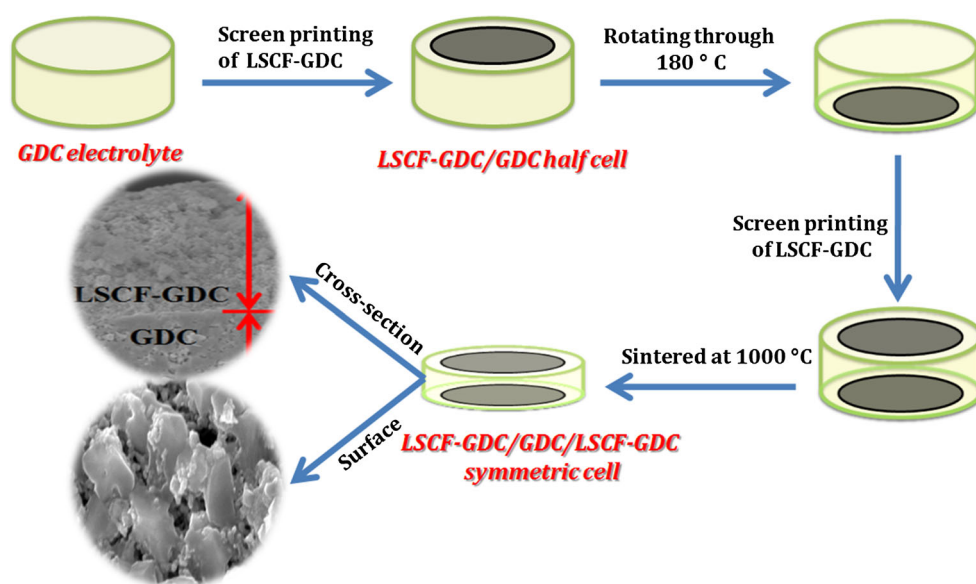
### 2.2 Fabrication of anode supported NiO-GDC/GDC/LSCF-GDC cell

In anode supported SOFCs, NiO-GDC (30:70 wt%) was prepared by the physical mixing of combustion synthesized powder and compacted under the hydraulic pressure of 83 Mpa. Thereafter, the NiO-GDC/GDC half cells were fabricated by spraying the GDC precursor onto NiO-GDC. The substrate temperature and precursor concentration maintained during the experiments were 300 °C and 0.025 M, respectively. To remove the excess water and stresses within the films, the half cells were heat treated at 450 °C for 5 h. Subsequently, the complete cells were formed by screen printing the LSCF-GDC (50:50 wt%) slurry onto GDC. The entire cells were sintered at 1000 °C for 2 h.

### 2.3 Characterization

For determination of chemical compatibility amongst electrode/electrolyte, the electrolyte supported symmetric

**Fig. 1** A schematic representation of the fabrication of symmetric SOFC with GDC as a framework



SOFCs have been characterized with X-ray diffractometer (XRD, Bruker). The morphological study was done with the atomic force microscopy (AFM, ICON analytical) and scanning electron microscopy (SEM, JEOL JSM 6360) techniques. The electrochemical impedance of symmetrical cells was carried out by using the Solartron 1260 impedance/gain phase analyzer. The frequency was swept from 1 mHz to 10 MHz with an AC excitation amplitude of 100 mV. The measurements were performed in air atmosphere and in the temperature range of 600–800 °C. The overall performance of cell was evaluated by using the probostat instrument in the range of 450–600 °C.

### 3 Results and discussion

#### 3.1 Chemical compatibility

Prior to performance measurement of cell through electrical conductivity, it is imperative to make sure whether all the cell components are chemically compatible with one another. Generally, the chemical compatibility is checked by studying X-ray diffraction pattern. Figure 2 shows the XRD pattern of LSCF-GDC composite cathode screen printed onto GDC and sintered at 1000 °C for 2 h. The pattern emphasizes that no chemical reaction occurred between the electrode and electrolyte to form the insulating phases like  $\text{SrZrO}_3$ ,  $\text{La}_2\text{ZrO}_7$  as in LSCF-YSZ composite [12]. Thus, the LSCF-GDC is found to be chemically stable upon the high temperature sintering [13]. The intense GDC peaks in LSCF-GDC/GDC are mainly due to the reflections from GDC particles in LSCF-GDC thick film rather than from substrate. Furthermore, nanocrystalline GDC have high surface area and sinterability [14], which

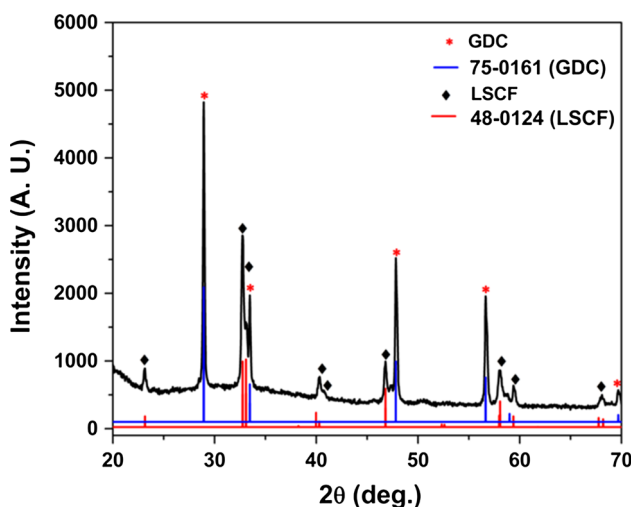


**Fig. 2** XRD pattern of LSCF-GDC composite cathode screen printed on GDC electrolyte

results into significant grain growth. This result is in validation with SEM, where large sized GDC particles are detected on the surface.

#### 3.2 Microstructural analysis

Figure 3a, b shows the surface scanning electron micrographs of GDC electrolyte and screen printed LSCF-GDC composite, while the cross-section of LSCF-GDC/GDC interface has been demonstrated in Fig. 3c. The substrate prepared through the conventional route does not get densify as per requirement, since it requires the temperature still higher than 1450 °C. However, the surface of GDC appears to be highly dense as the surface diffusion phenomenon is predominant at surface possessing higher surface energy than the interior. Also, Fig. 3a shows the non-uniform distribution of grains with the observation of some pores. The cross-sectional SEM shows that the film has good adherence and it provides perfect electrode/electrolyte interface, which minimizes the polarization resistance in association with imperfection at the interface. The thickness of electrode was calculated from the cross-section SEM and it is 15  $\mu\text{m}$ .

Furthermore, the surface analysis of composite thick films shows uniform distribution of GDC particles with significant grain growth. This abnormal grain growth may be caused by higher sinterability and high surface area of nanocrystalline GDC. Besides, the grain growth of GDC is enhanced by the presence of Co and Fe from LSCF [13, 15]. However, the composite thick films are appeared to be more porous in nature. This porous nature is elucidated in terms of roughness measurements carried out with atomic force microscope as shown in Fig. 3d and it is calculated within 2  $\mu\text{m}$  region. The roughness of LSCF-GDC composite thick film is about 0.843  $\mu\text{m}$ . Thus, the composite thick film appears to be much rougher. Typically, the grain size of GDC in composite thick film is 1  $\mu\text{m}$ .

#### 3.3 Electrochemical impedance of symmetric cell

The composite cathode has low electric conductivity at room temperature; the electrochemical impedance analysis of LSCF-GDC/GDC/LSCF-GDC symmetric cell was studied in the range of 600–800 °C and in air atmosphere. The obtained results were plotted and demonstrated in Fig. 4.

The Nyquist plots of LSCF-GDC/GDC/LSCF-GDC showed two semicircles followed by the resistance ( $R_0$ ) offered by the lead wire, silver contact, electrode and electrolyte. The semicircles were simulated with two  $R||CPE$  circuits in series with  $R_0$ . The first arc ( $R_1||CPE_1$ ) in high frequency region has capacitance of  $10^{-8} \text{ Fcm}^{-2}$ , attributing charge transfer process across the current

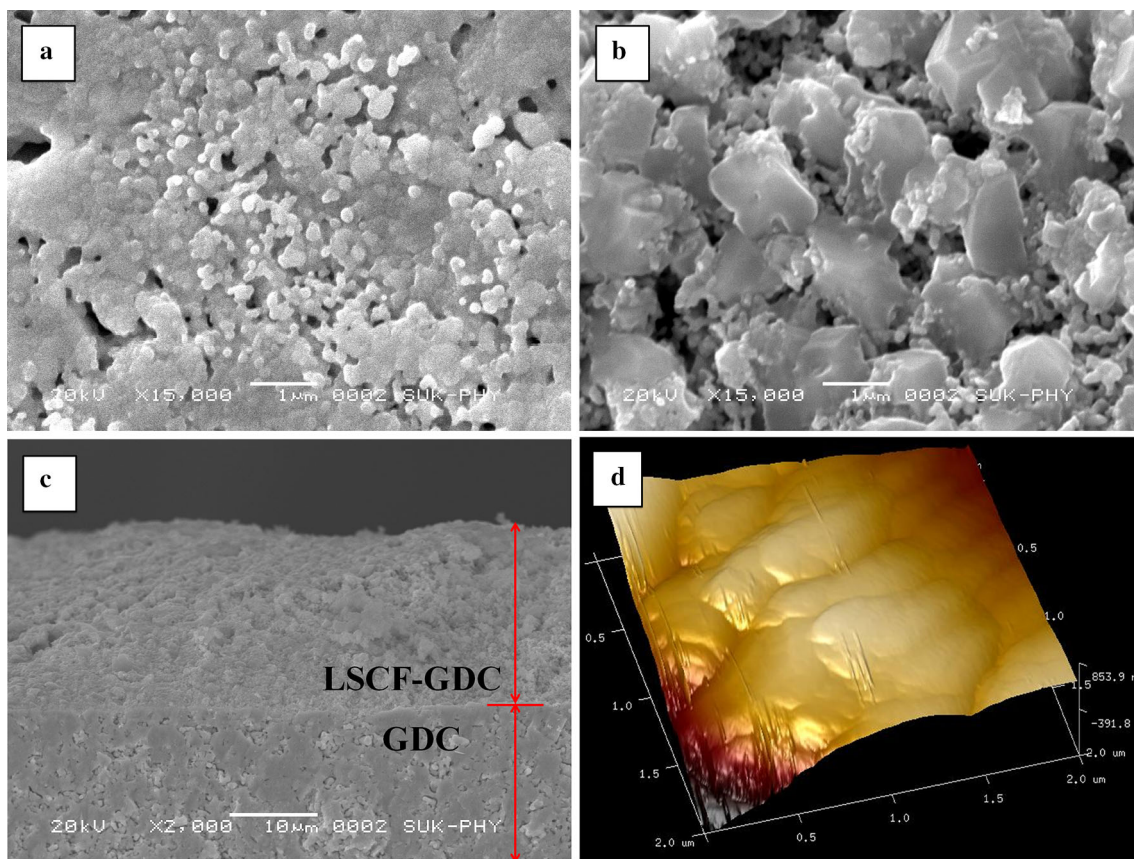


**Fig. 3** Surface SEM micrographs of **a** GDC substrate, **b** screen printed LSCF-GDC composite and **c** cross-section of LSCF-GDC/GDC interface, **d** 3D topography of screen printed LSCF-GDC composite

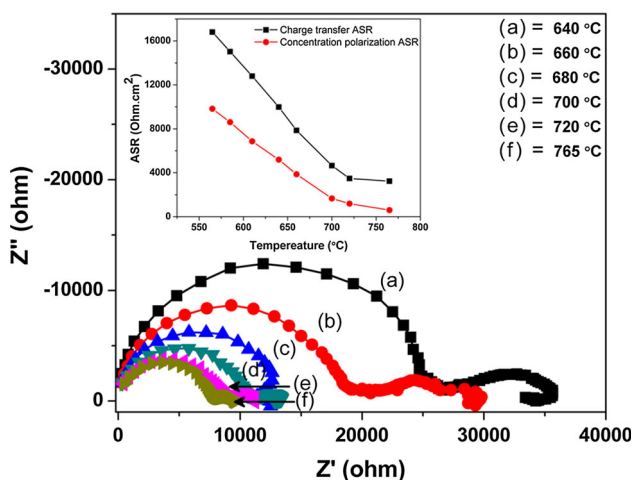


**Fig. 4** Electrochemical impedance spectra of the symmetric cell in air and at different operating temperatures

collector/electrode and electrode/electrolyte interface (charge transfer resistance). The second arc ( $R_2||CPE_2$ ) in lower region has capacitance of  $10^{-2} \text{ Fcm}^{-2}$  and can be ascribed to adsorption and dissociation of oxygen molecules followed by electrochemical reduction and surface

diffusion of oxygen species (concentration polarization) [16]. In addition, there is observation of inward inductive tail at the low frequency side and this is caused by the porous nature of the electrodes where the oxygen gets reduced to the oxygen ion. The diameters of semicircles are observed to decrease with temperature, indicating relaxation of these processes. The total polarization resistance associated with the composite cathode is determined from the difference of low and high frequency intercepts on the real axis, which is sum of the diameters of two semicircles. The cell with composite cathode has different Nyquist plot than those of pure LSCF [17]. This may be due to the large particles of GDC, porous nature of electrodes and its lower electrical conductivity.

### 3.4 Current voltage measurement of SOFC unit cell

The NiO-GDC supported SOFC with GDC and LSCF-GDC fabricated through spray pyrolysis and screen printing technique is tested for their performance in 2% hydrogen mixed with argon and air at the respective electrodes. Figure 5 shows the cell performance recorded at the operating temperature of 450, 500, 550 and 600 °C. The OCV is observed to increase with temperature up to



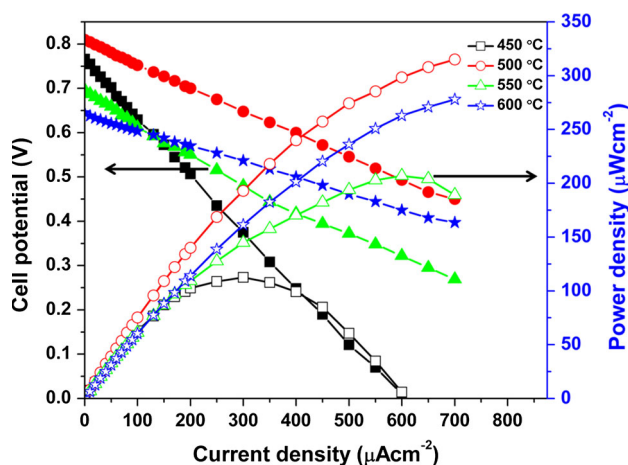


**Fig. 5** Performance of NiO-GDC/GDC/LSCF-GDC single cell under 2 % hydrogen mixed with argon and at different operating temperatures

500 °C, beyond which it decreases. The decrement may be due to the partial reduction of cerium from  $\text{Ce}^{+4}$  to  $\text{Ce}^{+3}$  in reducing atmosphere, which creates n-type conductivity and a current leak through the electrolyte [18, 19]. Also, the electrolyte thickness is low, the rise of temperature beyond the 500 °C resulted into the cracking of the electrolyte and hence the overall performance of SOFC gets reduced. The maximum OCV and power density is obtained at an operating temperature of 500 °C and are 0.81 V and  $315 \mu\text{Wcm}^{-2}$ , respectively. The OCV is found to decrease monotonically with rise of current density causing leakage of current through the electrolyte [20].

#### 4 Conclusions

Screen printing provides easy and cost effective technique to deposit the composite cathode on GDC electrolyte. The XRD patterns showed no intermediate phase formation thereby assuring the chemical compatibility of LSCF-GDC with GDC. The thickness of composite film is about 15  $\mu\text{m}$  and is observed to be porous in nature. The AFM roughness of LSCF-GDC thick film is about 0.843  $\mu\text{m}$ . Thus, such a porous and rough structure makes the availability of number active sites for electrochemical reaction. The

electrochemical processes occurred within the symmetrical cells get relaxed with rise of temperature. Furthermore, a complete cell with thin film electrolyte showed maximum powder density of  $315 \mu\text{Wcm}^{-2}$  at 500 °C.

**Acknowledgments** The work was supported by DRDO. One of the authors, Dr. Atul P. Jamale is thankful to University Grant Commission, New Delhi for its support through UGC meritorious fellowship.

#### References

1. C. Sun, R. Hui, J. Roller, J. Solid State Electrochem. **14**, 1125–1144 (2010)
2. H. Lv, Y. Wu, B. Huang, B. Zhao, K. Hu, Solid State Ion. **177**, 901–906 (2006)
3. G. Hua, X. Ding, W. Zhu, J. Li, J. Mater. Sci.—Mater. Electron. **26**, 3664–3669 (2015)
4. S.M. Haile, Acta Mater. **51**, 5981–6000 (2003)
5. P. Gannon, S. Sofie, M. Deibert, R. Smith, V. Gorokhovskiy, J. Appl. Electrochem. **39**, 497–502 (2009)
6. S. Hongyan, M.A. Wenhui, Y. Jie, C. Xiuhua, L. Hangsheng, J. Rare Earths **28**, 917–921 (2010)
7. H.A. Hamedani, M. Baniassadi, M. Khaleel, X. Sun, S. Ahzi, D. Ruchc, H. Garmestani, J. Power Sources **196**, 6325–6331 (2011)
8. J.P.P. Huijismans, Curr. Opin. Solid State Mater. Sci. **5**, 317–323 (2001)
9. A.P. Jamale, S.U. Dubal, S.P. Patil, C.H. Bhosale, L.D. Jadhav, Appl. Surf. Sci. **286**, 78–82 (2013)
10. A.P. Jamale, S. Shanmugam, C.H. Bhosale, L.D. Jadhav, Mater. Sci. Semicond. Process. **40**, 855–860 (2015)
11. L.D. Jadhav, M.G. Chourashiya, A.P. Jamale, A.U. Chavan, S.P. Patil, J. Alloys Compd. **506**, 739–744 (2010)
12. B.K. Lai, A.C. Johnson, H. Xiong, S. Ramanathan, J. Power Sources **186**, 115–122 (2009)
13. C.J. Fu, Q.L. Liu, S.H. Chan, X.M. Ge, G. Pasciak, Int. J. Hydrog. Energy **35**, 11200–11207 (2010)
14. D.H. Prasad, H.R. Kim, J.S. Park, J.W. Son, B.K. Kim, H.W. Lee, J.H. Lee, J. Alloys Compd. **495**, 238–241 (2010)
15. A. Mai, V.A.C. Haanappel, F. Tietz, D. Stover, Solid State Ion. **177**, 2103–2107 (2006)
16. S.F. Wang, Y.R. Wang, C.T. Yeh, Y.F. Hsu, S.D. Chyou, W.T. Lee, J. Power Sources **196**, 977–987 (2011)
17. A.P. Jamale, C.H. Bhosale, L.D. Jadhav, J. Alloys Compd. **623**, 136–139 (2015)
18. Y.W. Sin, K. Galloway, B. Roy, N.M. Sammes, J.H. Song, T. Suzuki, M. Awano, Int. J. Hydrog. Energy **36**, 1882–1889 (2011)
19. K.L. Duncan, K.T. Lee, E.D. Wachsman, J. Power Sources **196**, 2445–2451 (2011)
20. Z. Shao, S.M. Haile, Nature **431**, 170–173 (2004)